Journal Pre-proof

Nickel-refining fumes induce NLRP3 activation dependent on mitochondrial damage and ROS production in Beas-2B cells

Rui Xin, Yu-Lin Pan, Yue Wang, Sheng-Yuan Wang, Rui Wang, Bing Xia, Ru-Nan Qin, Yao Fu, Yong-Hui Wu

PII: S0003-9861(19)30517-X

DOI: https://doi.org/10.1016/j.abb.2019.108148

Reference: YABBI 108148

To appear in: *Archives of Biochemistry and Biophysics*

Received Date: 3 July 2019

Revised Date: 29 September 2019

Accepted Date: 9 October 2019

Please cite this article as: R. Xin, Y.-L. Pan, Y. Wang, S.-Y. Wang, R. Wang, B. Xia, R.-N. Qin, Y. Fu, Y.-H. Wu, Nickel-refining fumes induce NLRP3 activation dependent on mitochondrial damage and ROS production in Beas-2B cells, *Archives of Biochemistry and Biophysics* (2019), doi: https://doi.org/10.1016/j.abb.2019.108148.

This is a PDF file of an article that has undergone enhancements after acceptance, such as the addition of a cover page and metadata, and formatting for readability, but it is not yet the definitive version of record. This version will undergo additional copyediting, typesetting and review before it is published in its final form, but we are providing this version to give early visibility of the article. Please note that, during the production process, errors may be discovered which could affect the content, and all legal disclaimers that apply to the journal pertain.

© 2019 Published by Elsevier Inc.

Journal Pre-proof

Nickel-refining fumes induce NLRP3 activation dependent on mitochondrial damage and ROS production in Beas-2B cells

Rui Xin[1], Yu-Lin Pan[1], Yue Wang[1], Sheng-Yuan Wang[1], Rui Wang[1], Bing Xia[1], Ru-Nan Qin[1], Yao Fu[1], Yong-Hui Wu[1,*]

[1] Department of Occupational Health, School of Public Health, Harbin Medical University, Harbin City, Heilongjiang Province, China.

[1,*] Address correspondence to this author at: Department of Occupational Health, School of Public Health, Harbin Medical University, 157 Baojian Road, Nangang District, Harbin City, Heilongjiang Province, China 150086

Phone: +86-451-8750-2827; Fax: +86-451-8750-2827, E-mail: wuyonghui777@163.com.

Journal Pre-proof

Journal Pre-proof

Abstract

Nickel (Ni) is a silver-white transition metal that is widely used in the production field due to its unique physical and chemical properties. As a toxicant, long-term exposure to Ni can cause rhinitis, pneumonia and other respiratory inflammation. In the present study, we investigated the effect of particles extracted from Ni-refining fumes on cell viability, inflammation-related proteins and mitochondrial damage in human lung epithelial Beas-2B cells. The cells were exposed to Ni-refining fume particles for 24 h at concentrations of 0, 6.25, 12.50 and 25.00 μg/mL. The expression levels of the NACHT-LRR-PYD domains-containing protein 3 (NLRP3), caspase-1, nuclear factor kappa-light-chain-enhancer of activated B cells (NF-κB), interleukin (IL)-1β and tumor necrosis factor (TNF)-α protein in Beas-2B cells exposed to Ni-refining fume particles increased significantly. Downregulation of NLRP3 expression by siRNA decreased the content of IL-1β. During activation of NLRP3, the mitochondrial membrane potential (MMP) decreased, the opening rate of mitochondrial permeability transition pore (MPTP) increased, and the content of reactive oxygen species (ROS) increased. Using lipopolysaccharide (LPS) intervention as the positive control group, N-acetylcysteine (NAC, an effective ROS remover) acted as an inhibitor. After NAC reduced the level of ROS, activation of the NLRP3 inflammasome was significantly inhibited. Ni-refining fumes caused significant cytotoxicity, inflammation and mitochondrial damage in Beas-2B cells. The present study thus provides experimental support for the hypothesis that Ni-refining fumes cause inflammation by inducing ROS production in Beas-2B cells.

Keywords

Ni-refining fumes; NLRP3 inflammasome; Mitochondria; ROS.

Journal Pre-proof

Journal Pre-proof

Introduction

Nickel (Ni) is the second most abundant element in the core of the earth after the element iron. It is a silver-white metal with magnetism which easily forms alloys and compounds with other elements in nature in addition to its form as elemental nickel [1,2]. It has been determined that the toxicity of insoluble Ni compounds is much higher than that of soluble Ni compounds; for example, the toxicity of 20 μmol/L Ni_3S_2 is equivalent to that of 600 μmol/L $NiCl_2$ [3]. Because insoluble nickel compounds are phagocytosed into cells, depositing a large bolus of nickel into the cells compared to how nickel ions soluble nickel compounds deliver into cells [4]. When Ni ions enter a cell, free radicals are produced, resulting in cell membrane changes, cell injury and even death. The process of nickel refining has been classified by the International Agency for Research on Cancer (IARC) as a category I known human carcinogen [5]. Epidemiological investigations have determined that exposure on human workers to nickel compounds in the process of nickel refining, such as at Clydach, Wales, in the U.K., and other countries, have led to induction of nasal cancer and lung cancer in the exposed populations, and most of the patients who developed lung cancer had previously diagnosed pneumonia, rhinitis or other chronic inflammations of the respiratory system [6-8].

Inflammation is a series of complex physiological and pathological reactions caused by the harmful stimulation of the internal and external environment of the body tissues. It is a protective defense response, which is beneficial to the body by removing foreign substances, reducing damage and initiating repair [9]. Many cells of the body synthesize and secrete peptide-like factors collectively referred to as cytokines, such as interleukin (IL) factors, tumor necrosis factor (TNF) and others. Most studies of ILs have focused on the pro-inflammatory cytokine IL-1β, which plays an important role in immunity. The immunoregulatory inflammasome is the core link of inflammatory reactions, which is closely related to the secretion of

Journal Pre-proof

cytokines and tumors [10]. Further research has found that the inflammasome plays an important role in regulating cell death and apoptosis[11].

The inflammasome is a complex composed of polyproteins. The most characteristic and widely studied inflammasome is the NACHT-LRR-PYD domains-containing protein 3 (NLRP3) inflammasome. It has been confirmed that a variety of environmental crystals and particles, such as carbon nanotubes, can cause NLRP3 inflammasome activation *in vivo* and *in vitro* [12,13]. An increasing amount of clinical and experimental evidence suggests that the inflammatory response caused by activation of the NLRP3 inflammasome and the release of IL-1β is of particular significance in the pathogenesis of disease [14,15]. Studies have shown that IL-1β is produced as an inactive precursor that requires cleavage to be released from the cell and subsequently produce biological activity, while the related protein complex of the NLRP3 inflammasome may be responsible for regulating this process [16,17].

Several experiments have confirmed that changes in intracellular ion concentration and the content of reactive oxygen species (ROS) play an important role in the activation of the NLRP3 inflammasome, while inhibition of Ca^{2+} inflow/K^{+} outflow and decreased ROS production can block the activation of NLRP3 to a certain extent [18-21]. However, there is no general mechanism to explain the activation of the NLRP3 inflammasome, and the regulatory effect of ROS has not been consistently observed. Therefore, the specific mechanisms underlying inflammasome activation require further explanation.

In recent years, many studies have shown that the NLRP3 inflammasome plays an important role in the development of pulmonary diseases such as pulmonary infection, asthma, COPD and pulmonary fibrosis [10]. Most pathogens that cause respiratory infectious diseases can activate the NLRP3 inflammasome [16]. One study has shown that dermal exposure to Ni compounds can cause acute inflammation and allergic reactions in the occupational environment [22]. Long-term exposure to Ni may

lead to lung inflammation and eventually transformation into cancer [23]. The release of cytokines plays an important role in Ni-induced injury [24]. However, the specific molecular mechanism underlying the inflammatory response induced by NLRP3 has not been completely determined. Whether the NLRP3 inflammasome can be activated by Ni-refining fumes to induce an inflammatory response in normal human lung epithelial Beas-2B cells remains to be studied.

An analysis of the components of Ni-refining fumes was carried out using inductively coupled plasma mass spectrometry by our research group in a previous study [25]. The results showed that Ni-refining fumes were a mixture of micro-particles with several metals (Ni, Fe, Cu, Al and others) in the fumes, the highest content being Ni which accounted for 94.88% of total metals and was significantly higher than the other metals (Table 1). In previous studies by our research group, we demonstrated that Ni-refining fumes could induce oxidative stress, DNA damage [26] and inflammatory effects in NIH/3T3 cells [25]. In the current study, we aimed to determine if exposure to particles from Ni-refining fumes induced Beas-2B cell inflammation by activating the NLRP3 inflammasome. Inflammasome activation was observed by detecting inflammatory-related proteins, cytokines, mitochondrial changes and other indicators to explore the molecular mechanisms of NLRP3 inflammasome activation induced by Ni-refining fumes. We used mitochondria as mediators to elucidate the relationship between inflammation and injury. N-acetylcysteine (NAC), an inhibitor of ROS, was used as an intervention to further explore the toxic mechanism of Ni in cells. Our goal was to provide a reliable scientific basis for the prevention and treatment of occupational hazards in Ni refineries.

Materials and Methods

Cell culture and treatments

Human lung epithelial Beas-2B cells were obtained from the Cell Bank of the Chinese Academy of Sciences. Beas-2B cells were derived from cultured human

bronchial epithelial cells following immortalization of them by transfection of the SV40 large T antigen into them, in the laboratory of Dr. Curtis C. Harris at the National Cancer Institute of the National Institutes of Health, USA [27]. In this experiment, the culturing procedures for these cells are the same from those of Dr. Harris' laboratory. Beas-2B cells were cultured in Dulbecco's Modified Eagle Medium (DMEM; Corning Incorporated, Corning NY, USA). The culture medium contained 10% fetal bovine serum (FBS; GIBCO, Grand Island, NY, USA) and 1% penicillin/streptomycin. Cells were maintained at 37°C as monolayers in a humidified atmosphere containing 5% CO_2. When the cells reached 80% confluence, they were washed with prewarmed phosphate-buffered saline (PBS; GIBCO, Grand Island, NY, USA). The cells in the positive control group were primed with 25 μg/mL ultrapure lipopolysaccharides (LPS; Sigma-Aldrich, St. Louis, MO, USA) for 5 h. The cells in the negative control group were preincubated with ROS scavenger N-acetylcysteine (NAC, 5 mM; Sigma-Aldrich, St. Louis, MO, USA) for 30 min before exposure to Ni-refining fume particles. The stock suspensions were sonicated for 10 min and diluted to the appropriate concentrations before cell treatments. The cells were then treated with suspensions of particles from Ni-refining fumes at different concentrations (0.00 μg/mL, 6.25 μg/mL, 12.50 μg/mL, 25.00 μg/mL) for 24 h.

Preparation of test materials

Ni-refining fumes were sampled from a refinery workshop at JILIN JIEN NICKEL INDUSTRY CO., LTD, Panshi City, Jilin Province, China. The method of sampling and collecting Ni-refining fumes is based on the National Occupational Health Standard *GBZ/T192: Method for determination of dust in the air of workplace* issued by the Ministry of Health of the People's Republic of China. Used the ICP-MS method to determine the exact composition of the Ni-refining fumes (Table 1). The fumes were ground in an agate mortar, and the diameter of the particles in the fumes was less than 5 μm in 99% of the particles. After sterilization by ultraviolet radiation

for 1 h, the particles were placed into phosphate-buffered saline (PBS), forming a liquid suspension for later use.

Chemicals, reagents and antibodies

Primary antibodies against caspase-1, nuclear factor kappa-light-chain-enhancer of activated B cells (NF-κB; p65 component) and NLRP3 were purchased from Cell Signaling Technology (Danvers, MA, USA). Antibodies against β-actin, horseradish peroxidase-labeled anti-mouse IgG (ZB-2305) and anti-rabbit IgG (ZB-2301) were obtained from ZSGB-BIO (Beijing, China). A Cell Counting Kit-8 (CCK-8) was purchased from Dojindo (Kumamoto, Japan). FITC (Fluorescein isothiocyanate) -conjugated goat anti-rabbit IgG secondary antibody and DAPI (4',6-Diamidino-2-Phenylindole, Dihydrochloride) dye were obtained from OriGene Technologies (Rockville, MD, USA). BCA protein assay kit and 2',7'-Dichlorodihydrofluorescein diacetate (DCFH-DA) assay kit were obtained from Beyotime Biotechnology (Shanghai, China). The calcein-AM staining solution and fluorescent probe JC-1 were from Genmed Scientifics Inc. (Wilmington, DE, USA). TRIzol reagent was purchased from Invitrogen (Carlsbad, CA, USA) and a ReverTra Ace® qPCR RT Kit was purchased from Toyobo (Osaka, Japan).

Cell viability assessment by CCK-8 assay

To assess cell viability, Beas-2B cells in logarithmic growth phase were seeded into 96-well plates (1×10^4 cells/well) and exposed to particles from Ni-refining fumes at concentrations of 0.00 μg/mL, 6.25 μg/mL, 12.50 μg/mL, 25.00 μg/mL and 50.00 μg/mL for 24 h. Each group included six replicates. At the end of the incubation period, 10 μL of CCK-8 solution were added into each well and incubated for 2–4 h. The absorbance was read at a wavelength of 490 nm with an enzyme-linked immunosorbent assay (ELISA) reader at least three times. Cell viability was expressed as the relative survival rate calculated as the ratio of the absorbance of Ni-treated groups to the absorbance of the blank control group.

Cytokine assay

The release of cytokines into cell culture supernatants was detected by ELISA. IL-1β and TNF-α levels were detected using human IL-1β and human TNF-α ELISA Kits (both from R&D Systems, Inc., USA), following the manufacturer's instructions.

RNA extraction, reverse transcription and real-time qPCR

Total RNA was extracted from Beas-2B cells by TRIzol reagent, and the extracted RNA samples were reverse-transcribed to cDNA using the ReverTra Ace® qPCR RT Kit. The cDNA was used as a template for real-time qPCR. The relative fold change in expression of the target normalized to expression of the corresponding control was calculated by the comparative Ct method. A list of primers was shown in Table 2.

Immunofluorescence Staining

After treatment with different concentrations of particles from Ni-refining fumes for specific durations, the cells were washed twice with PBS and then fixed with 4% paraformaldehyde for 30 min at room temperature before being washed again with PBS. A 0.1% Triton X-100 solution was added, and the cells were incubated for 30 min, then washed with PBS. BSA (2%) was added to the cells for 30 min, followed by PBS washing. Primary antibody against NLRP3 was added (1:50), and the cells were incubated at 4°C overnight and washed with PBS three times for 5 min per wash. Secondary anti-Cy3 (goat anti-rabbit IgG) antibody was added, and the cells were incubated at 37°C for 1 h, then washed with PBS three times for 5 min per wash. The nucleus was stained with DAPI for 10 min, and the cells were washed 3 times with PBS for 5 min per wash. Images were captured under an inverted fluorescence microscope (CX41-FS, Olympus, Japan) and digitized.

Western blot analysis

Cells treated with various concentrations of particles from Ni-refining fumes for

24 h were washed twice with PBS and lysed in cell RIPA lysis buffer containing 1 mM PMSF on ice for 50 min. The cell suspension was then centrifuged for 10 min at 12,000 rpm at 4°C and the supernatant was collected. Total protein concentration was determined using the BCA Protein Assay kit. Aliquots containing 50 μg of protein from each group were separated by 15% (w/v) SDS polyacrylamide gels and transferred to polyvinylidene difluoride membranes. The membranes were blocked with 5% non-fat milk/BSA in Tris-buffered saline containing 0.1% Tween 20 (TBST) for 30 min at 37°C, then incubated with rabbit-polyclonal primary antibodies against caspase-1 (1: 1,000), NF-κB (p65) (1: 1,000), NLRP3 (1: 1,000) and β-actin (1: 1,000) overnight at 4°C. Blots were washed three times with TBST, followed by 30 min incubation with the appropriate goat anti-rabbit alkaline phosphatase (AP)-conjugated secondary antibodies (1: 2,000). The antibody-reactive bands were monitored by stabilized substrate for AP and quantified by densitometry using ChemiAnalysis image analysis software (Clinx Science Instruments, China). β-actin was used as an internal control.

Determination of mitochondrial membrane potential (MMP)

The MMP was analyzed using the fluorescent probe JC-1, which has two staining spectra. Under normal conditions, the dye forms aggregates in the mitochondrial membrane, exhibiting red fluorescence. When the membrane potential is lost, monomeric JC-1 forms in the cytosol, resulting in green fluorescence. Beas-2B cells were stained with JC-1 staining solution for 20 min at 37°C and then washed twice with cleaning solution. After resuspension in fresh culture medium, the absorbance under emission wavelength of 520/590 nm was read immediately on a microplate reader with an excitation filter of 490 nm, and the data were used to calculate the fluorescence ratio. After observation under a fluorescence microscope, a decrease in red fluorescence intensity was considered an indicator of MMP loss.

Detecting the opening rate of mitochondrial permeability transition pore

(MPTP)

Beas-2B cells (1×10^4 cells/well) were inoculated into a black 96-well plate. After 24 h exposure to Ni, the cells were washed three times with sterile PBS, followed by addition of 500 μL of cleaning solution into each well, covering the surface of the well before removal. Then, 100 μL pre-prepared calcein-AM staining solution was added along the pore wall and incubated at 37°C in the dark for 20 min. The staining solution was carefully removed and preheated cleaning solution (37°C) was added twice along the wall of the well. After addition of the fluorescent enzyme marker, absorbance was measured at an excitation wavelength of 488 nm and emission wavelength of 505 nm. The relative fluorescence units were calculated according to the fluorescence intensity to determine the extent of MPTP opening. A decrease in fluorescence intensity indicated that the opening of the MPTP had increased.

Intracellular ROS detection

The content of ROS in cells was detected by DCFH-DA assay. After treatment, the cells were incubated with DCFH-DA at 37°C for 30 min. Subsequently, the fluorescence was measured at 488 nm for excitation and 525 nm for emission.

Statistical analysis

The statistical package SPSS, version 18.0 for Windows (SPSS, IBM, Armonk, NY, USA) was used for statistical analysis. Results are presented as means ± standard error of the mean (SEM). Comparisons between groups were analyzed using one-way analysis of variance, and further pairwise comparisons were performed using the least significant difference t-test. A P value ≤ 0.05 indicated statistical significance.

Results

Characterization of Ni-refining fumes

Transmission electron microscopy analysis showed that the particle size in

Ni-refining fumes varied, the shapes were irregular, and there were hollow tetragonal or circular particles in the middle. The minimum size was 0.5 μm, the maximum diameter was 7 μm, but most of the particle sizes were concentrated in the range of 1-3 μm, suggesting that they could exert a toxic effect on nasal hair and cilium of the upper respiratory tract and enter into alveolar tissue and cells (Figure 1).

Ni-refining fumes induce cytotoxicity and cytokine secretion in Beas-2B cells

To evaluate the cytotoxicity of Ni-refining fumes, we first exposed Beas-2B cells to various doses of particles from Ni-refining fumes (0.00 μg/mL, 6.25 μg/mL, 12.50 μg/mL, 25.00 μg/mL and 50.00 μg/mL) for 24 h. The absorbance was determined by CCK-8 assay, and relative activity was assumed to reflect the toxic effect of Ni-refining fumes. We found that Ni-refining fume particles inhibited cell viability in a dose-dependent manner (Figure 2). To investigate the inflammatory potential of Ni-refining fumes, we examined cytokine release in the cell culture supernatants. The secretion of IL-1β and TNF-α in the culture supernatants was measured by ELISA and was found to be significantly increased in a dose-dependent manner after Ni stimulation (Figure 3A, B). Compared with the control group, the expression of IL-1β and TNF-α mRNA in the group exposed to Ni-refining fumes was significantly increased ($P<0.05$). However, the mRNA levels of IL-1β and TNF-α in the low concentration group did not increase with the increase in Ni-refining fumes concentration, and there was no significant difference between the two groups (Figure 3C, D).

Ni-refining fumes induce NLRP3 inflammasome activation in Beas-2B cells

The fluorescence intensity of NLRP3 protein significantly increased in the groups exposed to 12.50 μg/mL and 25.00 μg/mL of Ni-refining fumes, indicating that Ni enhanced NLRP3 protein expression in Beas-2B cells (Figure 4A). However, fluorescently- labeled NLRP3 protein was not observed in the control group, indicating that it was in a resting state under normal conditions, and that the basic

content of NLRP3 in the cells was insufficient to constitute an inflammatory complex to activate inflammatory expression.

We also used western blots to detect the expression of NLRP3 inflammasome-associated proteins in Beas-2B cells. Compared to the control group, with the increase in Ni-refining fumes concentration, the expression of NLRP3, caspase-1 and NF-κB (p65) proteins was increased in a dose-dependent manner (Figure 4B, C, E, F). At the same time, the expression level of NLRP3 mRNA was also increased compared with the control group (Figure 4D). This trend coincided with protein expression observed by immunofluorescence, indicating that Ni-refining fumes activated the NLRP3 inflammasome in Beas-2B cells.

Ni-refining fumes-induced cytokine secretion is dependent on NLRP3 inflammasome activation in Beas-2B cells

To further clarify the effect of the NLRP3 inflammasome on the release of inflammatory cytokines such as IL-1β, we downregulated NLRP3 expression in cells using siRNA (Figure 5A, B, C). NLRP3 siRNA successfully inhibited NLRP3 protein and mRNA expression compared to the control group. At the same time, after exposure to Ni-refining fume particles (25.00 μg/mL) for 24 h, ELISA results showed that NLRP3 siRNA significantly reduced IL-1β content in the cells (Figure 5D; $P<0.05$). These results confirmed that the NLRP3 inflammasome mediated the release of IL-1β inflammatory cytokines from Beas-2B cells caused by Ni-refining fumes, which in turn induced the inflammatory effect on Beas-2B cells.

Ni-refining fumes induced mitochondria damage in Beas-2B cells

The ultrastructure of Beas-2B cells was observed by transmission electron microscopy. As shown in Figure 6A, in the normal control group, multiple mitochondria were observed in Beas-2B cells. These mitochondria displayed normal morphology and size, and complete boundaries, mitochondrial ridges and intimal

Journal Pre-proof

structures were clearly visible; the mitochondrial morphology was full and no damage or deformation was observed. After exposure to 12.50 μg/mL of Ni-refining fume particles for 24 h, mitochondrial morphology changed significantly, becoming irregular and nonuniform. Swelling of internal mitochondrial ridges and intimal structures was observed, and foaming began to appear. After exposure to 25.00 μg/mL Ni-refining fume particles for 24 h, this change was even more obvious. The mitochondria were unable to maintain steady state, and the internal structure began to crack and break, showing a large degree of vacuolization, with visible particles of Ni-refining fumes were phagocytosed into the Beas-2B cells. These structural changes suggested that Ni-refining fumes had caused mitochondrial damage in Beas-2B cells.

Mitochondrial MMP was labeled with JC-1 dye and observed under a fluorescence microscope. The decrease in red fluorescence intensity indicated that the degree of MMP dissipation had increased and that damage to mitochondrial function had occurred. As shown in Figure 6B, in Beas-2B cells exposed to 12.50 μg/mL and 25.00 μg/mL Ni-refining fumes for 24 h, the red fluorescence intensity compared to control cells decreased gradually with increasing Ni concentration, indicating increasing loss of mitochondrial MMP. At the same time, the morphology of cells in the 25.00 μg/mL Ni-refining fumes group also changed obviously. We measured and calculated the fluorescence ratio of MMP and the opening rate of MPTP using a fluorescence enzyme-labeling instrument. As shown in Figure 6C and D, compared with the control group, the MMP in the 25.00 μg/mL Ni-refining fumes group decreased while the MPTP opening rate increased. These differences were statistically significant (P<0.05). The results suggested that exposure to Ni-refining fumes decreased MMP, increased the MPTP opening rate and damaged the function of mitochondrial in Beas-2B cells.

NLRP3 activation by Ni-refining fumes is dependent on ROS production in Beas-2B cells

As an effective ROS scavenger, NAC was used as an intervention under the same concentrations of Ni-refining fume particles used in the previous experiments. The results of ROS absorbance measurements using a fluorescence microplate reader are shown in Figure 7A, B. Compared with the 25.00 μg/mL of Ni-refining fumes group, NAC intervention significantly reduced the excessive production of ROS caused by Ni (P<0.05).

After exposure to 25.00 μg/mL of Ni-refining fumes for 24 h, Beas-2B cells were treated with NAC to detect the activation of NLRP3 inflammasome-associated proteins and inflammatory cytokines. Western blot results are shown in Figure 8A, B, C, D. Compared with the control group, the expression of NLRP3, caspase-1 and NF-κB (p65) proteins in the 25.00 μg/mL Ni-refining fumes group increased significantly. The protein expression levels of NLRP3 and NF-κB (p65) in the NAC group were significantly lower than in the 25.00 μg/mL Ni-refining fumes group (P<0.05), while NAC had no significant effect on the protein expression of caspase-1. The results of RT-qPCR are shown in Figure 8E. Compared with the control group, mRNA levels of NLRP3, caspase-1 and NF-κB (p65) were significantly increased. After treatment with NAC, compared with the 25.00 μg/mL Ni-refining fumes group, the mRNA expression levels were all significantly decreased (P<0.05).

The results of ELISA are shown in Figure 8F. Compared with the control group, the IL-1β content in the cells was significantly increased. After NAC intervention, the IL-1β content in the cells was significantly lower than in the 25.00 μg/mL Ni-refining fumes group (P<0.05). This result was consistent with changes in NLRP3 inflammasome-associated protein and mRNA expression levels. Notably, the mRNA expression level of caspase-1 in the NAC intervention group was lower than in the 25.00 μg/mL Ni-refining fumes group, but caspase-1 protein expression did not change significantly, suggesting posttranscriptional regulation of caspase-1 mRNA.

These results suggested that NAC could effectively antagonize the increase and

Journal Pre-proof

activation of NLRP3 inflammasome-associated proteins and mRNA expression in Beas-2B cells induced by Ni-refining fumes exposure, thus inhibiting inflammasome activation and reducing the secretion of inflammatory cytokines, which diminished the inflammatory reaction in the cells.

Discussion

Many case studies showed that exposure of humans to nickel compounds, particularly insoluble nickel compounds in nickel ores, leads to nasal and lung tumors [6-8,28-30]. It is clear that the toxicological properties of Ni and its compounds are important challenges in risk assessment and require implementation of preventive measures for workers exposed to Ni. To date, most of the studies examining Ni have used pure Ni compounds as test substances. However, this is not consistent with the actual exposure of Ni refinery workers to Ni dust. Nickel is often used with other heavy metals (chromium or cadmium) and is rarely used alone. Therefore, we used Ni-refining fumes collected on site in the Ni-refining workshop to simulate the real-world exposure environment of the occupational population. Inhalation through the respiratory tract is the main form of exposure to Ni, and lung epithelial cells are the primary target for Ni exposure. In this experiment, we chose Beas-2B as the target cells to more accurately reflect the toxic effects of Ni-refining fumes on the lungs.

The inflammatory response plays an important role in the occurrence and development of a variety of acute and chronic lung injury diseases [31]. Studies have found that the use of NiNPs (nickel nanoparticles) leads to increased environmental and occupational exposures, which are associated with increased risk of lung inflammation, pneumonia and respiratory cancer [32,33]. IL-1β is an important proinflammatory mediator which is mainly produced during infection, injury or in the

Journal Pre-proof

immune response and is the central mediator of the inflammatory response. NF-κB is a transcription factor involved in the production of cytokines, the development of cancer and the response to inflammatory stimuli.

In this study, we found that Ni-refining fume particles can be phagocytosed by Beas-2B cells, resulting in a decrease in cell activity which was dose-dependent on the concentration of Ni. At the same time, we tested the effect of fume particles on release of inflammatory cytokines such as IL-1β, TNF-α and NF-κB. The results indicated that Ni-refining fume particles can be taken up and transported by the cells, and may cause inflammatory reactions in the cells through the NF-κB pathway, resulting in toxic effects, cellular inflammatory reactions, damage to cells and inhibition of cell viability. However, RT-qPCR results showed that the mRNA levels of IL-1β mRNA and TNF-α were not significantly affected by some concentrations of fume particles (6.25 μg/mL and 12.50 μg/mL). This result suggested that the secretion and release of IL-1β and TNF-α in Beas-2B cells induced by low concentrations of Ni-refining fumes may not depend solely on changes in transcription.

The NLRP3 inflammasome is an important subject of cellular inflammation research. NLRP3, apoptosis-associated speck-like protein containing CARD (ASC) and caspase-1 are important components of the NLRP3 inflammasome [12-14]. At resting state, caspase-1 exists in the form of inactive pro-caspase-1, and the NLRP3 protein content in cells is extremely low [16]. As an intracellular signaling platform, NLRP3 inflammasome activation can induce a large number of pro-inflammatory cytokines such as IL-1β and TNF-α [34].

In the present experiments, we found that the NLRP3 inflammasome could be activated by an increased concentration of Ni-refining fumes. In this process, caspase-1 mRNA was increased, as was protein expression. When we downregulated the expression of NLRP3 protein by siRNA, the expression of NLRP3 and the secretion of IL-1β induced by Ni-refining fumes was effectively inhibited. These

results suggested that the NLRP3 inflammasome was involved in mediating the inflammatory response of Beas-2B cells induced by Ni-refining fumes. Therefore, blocking or inhibiting the activation of NLRP3 may be a novel target for the treatment of inflammatory diseases caused by Ni. Although the NLRP3 inflammasome has been shown to be potentially important in the pathogenesis of several diseases, details of the mechanism underlying its activation through various stimulants have not been reported.

Recently, many experiments have confirmed that the change in intracellular ROS content plays an important role in the activation of the NLRP3 inflammasome, with the decrease in ROS production blocking activation of NLRP3 [18-20]. Mitochondria are important sources of cellular ROS during oxidative stress [35-37]. Excessive ROS production by abnormal mitochondria may be directly related to activation of the NLRP3 inflammasome. In a previous study from our research group, we found that Ni-smelting fumes caused oxidative damage to NIH/3T3 cells and decreased cell activity, which was closely related to mitochondrial function [38]. In the present study, we found that with the increase in the concentration of Ni-refining fumes, the intracellular ROS content increased significantly. At the same time, through transmission electron microscopy, we observed obvious swelling in the organelles of the mitochondria, which suggested that the mitochondria were damaged. The results of fluorescence analysis showed that as the concentration Ni-refining fumes increased, the number of open MPTPs increased while the MMP level gradually decreased. These results suggested that Ni-refining fumes may regulate the NLRP3 inflammasome through excessive production of ROS induced by damage to mitochondria.

Therefore, we believe that Ni-refining fumes induce mitochondrial dysfunction and the resulting ROS overproduction is the most likely signal to activate the NLRP3 inflammasome in Beas-2B cells (Figure 9). However, it cannot be ruled out that

Ni-refining fumes may cause lysosomal damage in Beas-2B cells, acting as simple particles to activate K^+ channels and subsequently the NLRP3 inflammasome [39,40]. Thus, the molecular mechanism regulating inflammasome activation by Ni-refining fumes in Beas-2B cells may not be a single pathway; rather, Beas-2B cells may integrate many downstream activation signals and activate the inflammasome via a common signaling pathway.

Conclusion

This study is the first to our knowledge to report that exposure to Ni-refining fume particles induced Beas-2B cell inflammation by activating the NLRP3 inflammasome. Our results showed that the NLRP3 inflammasome-mediated inflammatory response was one of the major molecular mechanisms inducing Beas-2B cytotoxicity after exposure to Ni-refining fumes, which may be helpful in explaining the association between inflammation and tumorigenesis. Blocking or inhibiting the activation of NLRP3 and protecting mitochondria with antioxidant and anti-inflammatory drugs may inhibit the inflammatory response and provide an effective strategy for antagonizing the damaging effect of Ni-refining fumes on cell viability. Our results may also help explain the specific molecular mechanisms linking chronic respiratory inflammation and tumors caused by exposure to Ni-refining fumes in occupational populations. Finally, this study provides a rationale and strategy for the protection and medical treatment of occupational populations exposed to Ni-refining fumes.

Acknowledgements

The author(s) wish to thank all those who have contributed to this study.

Declaration of Conflicting Interests

The author(s) declared no potential conflicts of interest with respect to the research, authorship, and/or publication of this article.

Journal Pre-proof

Funding

The author(s) disclosed receipt of the following financial support for the research, authorship, and/or publication of this article: This work was supported by National Natural Science Foundation of China (grant no. 81673138).

References

1. Freitas M, Barcellos-de-Souza P, Barja-Fidalgo C, Fernandes E. Nickel induces apoptosis in human neutrophils. *Biometals*. 2013;26(1):13-21.

2. Kročková JZ, Massányi P, Sirotkin AV, Pivko J, Makarevich AV, Lukáč N, Capcarová M, Toman R, Poláková Z. Nickel induced structural and functional alterations in mouse Leydig cells in vitro. *J Trace Elem Med Biol*. 2011;25(1):14-18.

3. Das KK, Das SN, Dhundasi SA. Nickel, its adverse health effects & oxidative stress. *Indian J Med Res.*2008;128(14):412-425.

4. Kuo CY, Wong RH, Lin JY, Lai JC, Lee H. Accumulation of chromium and nickel metals in lung tumors from lung cancer patients in Taiwan. *J Toxicol Environ Health.* 2006;69(14):1337-1344.

5. International Agency for Research on Cancer, IARC Monographs on the Evaluation of Carcinogenic Risks to Humans. Review of Human Carcinogens. (2012).

6. Sivulka DJ, Seilkop SK, Lascelles K, Conard BR, Jones SF, Collinson EC. Reconstruction of historical exposures at a Welsh nickel refinery (1953-2000). *Ann Occup Hyg.* 2014;58(6):739-760.

7. Grimsrud TK, Peto J. Persisting risk of nickel related lung cancer and nasal cancer among Clydach refiners. *Occup Environ Med.* 2006;63(5):365-366

8. Grimsrud TK, Berge SR, Resmann F, Norseth T, Andersen A. Assessment of

historical exposures in a nickel refinery in Norway. *Scand J Work Environ Health.* 2000;26(4):338-345.

9. Qian Q. Inflammation: A Key Contributor to the Genesis and Progression of Chronic Kidney Disease. *Contrib Nephrol.* 2017;191:72-83.

10. Kim RY, Pinkerton JW, Gibson PG, Cooper MA, Horvat JC, Hansbro PM. Inflammasomes in COPD and neutrophilic asthma. *Thorax.* 2015;70(12):1199-1201.

11. Schroder K, Tschopp J. The inflammasomes. *Cell.* 2010;140(6):821-832.

12. Kingsbury SR, Conaghan PG, McDermott MF. The role of the NLRP3 inflammasome in gout. *J Inflamm Res*. 2011;4:39-49.

13. Lee HM, Kim JJ, Kim HJ, Shong M, Ku BJ, Jo EK. Upregulated NLRP3 inflammasome activation in patients with type 2 diabetes. *Diabetes*. 2013;62(1):194-204.

14. Amaral FA, Costa VV, Tavares LD, Sachs D, Coelho FM, Fagundes CT, Soriani FM, Silveira TN, Cunha LD, Zamboni DS, Quesniaux V, Peres RS, Cunha TM, Cunha FQ, Ryffel B, Souza DG, Teixeira MM. NLRP3 inflammasome-mediated neutrophil recruitment and hypernociception depend on leukotriene B(4) in a murine model of gout. *Arthritis Rheum.* 2012;64(2):474-484.

15. Hussain S, Sangtian S, Anderson SM, Snyder RJ, Marshburn JD, Rice AB, Bonner JC, Garantziotis S. Inflammasome activation in airway epithelial cells after multi-walled carbon nanotube exposure mediates a profibrotic response in lung fibroblasts. *Part Fibre Toxicol*. 2014;11:28.

16. Yazdi AS, Guarda G, Riteau N, Drexler SK, Tardivel A, Couillin I, Tschopp J. Nanoparticles activate the NLR pyrin domain containing 3 (Nlrp3) inflammasome and cause pulmonary inflammation through release of IL-1alpha and IL-1beta.

Proc Natl Acad Sci U S A. 2010;107(45):19449-19454.

17. Fang L, Moore XL, Dart AM, Wang LM. Systemic inflammatory response following acute myocardial infarction. *J Geriatr Cardiol*. 2015;12(3):305-312.

18. Liu J, Qu W, Kadiiska MB. Role of oxidative stress in cadmium toxicity and carcinogenesis. *Toxicol Appl Pharmacol*. 2009;238(3):209-214.

19. Dong W, Simeonova PP, Gallucci R, Matheson J, Flood L, Wang S, Hubbs A, Luster MI. Toxic metals stimulate inflammatory cytokines in hepatocytes through oxidative stress mechanisms.*Toxicol Appl Pharmacol*. 1998;151(2):359-366.

20. Olszowski T, Baranowska-Bosiacka I, Gutowska I, Chlubek D. Pro-inflammatory properties of cadmium. *Acta Biochim Pol*. 2012;59(4):475-482.

21. Morimoto Y, Hirohashi M, Ogami A, Oyabu T, Myojo T, Hashiba M, Mizuguchi Y, Kambara T, Lee BW, Kuroda E, Tanaka I. Expression of cytokine-induced neutrophil chemoattractant in rat lungs following an intratracheal instillation of micron-sized nickel oxide nanoparticle agglomerates. *Toxicol Ind Health*. 2014;30(9):851-860.

22. Zhao J, Shi X, Castranova V, Ding M. Occupational toxicology of nickel and nickel compounds. *J Environ Pathol Toxicol Oncol*. 2009;28(3):177-208.

23. Capasso L, Camatini M, Gualtieri M. Nickel oxide nanoparticles induce inflammation and genotoxic effect in lung epithelial cells. *Toxicol Lett*. 2014;226(1):28-34.

24. Bechara R, Antonios D, Azouri H, Pallardy M. Nickel Sulfate Promotes IL-17A Producing CD4+ T Cells by an IL-23-Dependent Mechanism Regulated by TLR4 and Jak-STAT Pathways. *J Invest Dermatol*. 2017;137(10):2140-2148.

25. Qin RN, Wang Y, Wang SY, Xia B, Xin R, Li C, Wu YH, Nickel-refining dust regulates the expression of inflammatory factors in NIH/3T3 cells, *Toxicol Ind*

Health. 2019;35:239-247.

26. Wang Y, Wang SY, Jia L, Zhang L, Ba JC, Han D, Yu CP, Wu YH, Nickel-Refining Fumes Induced DNA Damage and Apoptosis of NIH/3T3 Cells via Oxidative Stress. *Int J Environ Res Public Health*. 2016;13(7):629.

27. Reddel RR, Ke Y, Gerwin BI, McMenamin MG, Lechner JF, Su RT, Brash DE, Park JB, Rhim JS, Harris CC. Transformation of human bronchial epithelial cells by infection with SV40 or adenovirus-12 SV40 hybrid virus, or transfection via strontium phosphate coprecipitation with a plasmid containing SV40 early region genes. *Cancer Res.* 1988; 48:1904-1909.

28. Costa M, Klein C. Nickel carcinogenesis, mutation, epigenetics, or selection. *Environ Health Perspect*. 1999;107(9):A438-A439.

29. Bolek EC, Erden A, Kulekci C, Kalyoncu U, Karadag O. Rare occupational cause of nasal septum perforation: Nickel exposure. *Int J Occup Med Environ Health*. 2017;30(6):963-967.

30. Chen QY, DesMarais T, Costa M. Metals and Mechanisms of carcinogenesis. *Annu Rev Pharmacol Toxicol*. 2019;59:537-554.

31. Yamano T, DeCicco LA, Rikans LE. Attenuation of cadmium-induced liver injury in senescent male fischer 344 rats: role of Kupffer cells and inflammatory cytokines. *Toxicol Appl Pharmacol*. 2000;162(1):68-75.

32. Falcone LM, Erdely A, Salmen R, Keane M, Battelli L, Kodali V, Bowers L, Stefaniak AB, Kashon ML, Antonini JM, Zeidler-Erdely PC. Pulmonary toxicity and lung tumorigenic potential of surrogate metal oxides in gas metal arc welding-stainless steel fume: Iron as a primary mediator versus chromium and nickel. *PLoS One*. 2018;13(12):e0209413.

33. Morgan LG, Usher V. Health problems associated with nickel refining and

use. *Ann Occup Hyg*. 1994;38(2):189-198.

34. Dzierba AL, Abel EE, Buckley MS, Lat I. A review of inhaled nitric oxide and aerosolized epoprostenol in acute lung injury or acute respiratory distress syndrome. *Pharmacotherapy*. 2014;34(3):279-290.

35. Maiti P, Gregg LC, McDonald MP. MPTP-induced executive dysfunction is associated with altered prefrontal serotonergic function. *Behav Brain Res.* 2016;298(Pt B):192-201.

36. Patil SP, Jain PD, Sancheti JS, Ghumatkar PJ, Tambe R, Sathaye S. Neuroprotective and neurotrophic effects of Apigenin and Luteolin in MPTP induced parkinsonism in mice. *Neuropharmacology.* 2014;86:192-202.

37. Sarkar S, Chigurupati S, Raymick J, Mann D, Bowyer JF, Schmitt T, Beger RD, Hanig JP, Schmued LC, Paule MG. Neuroprotective effect of the chemical chaperone, trehalose in a chronic MPTP-induced Parkinson's disease mouse model. *Neurotoxicology*. 2014;44:250-262.

38. Pan YL, Xin Rui, Wang SY, Wang Y, Zhang L, Yu CP, Wu YH. Nickel-smelting fumes induce mitochondrial damage and apoptosis, accompanied by decreases in viability, in NIH/3T3 cells. *Arch Biochem Biophys*. 2018; 660:20-28.

39. Szabo G, Csak T. Inflammasomes in liver diseases. *J Hepatol*. 2012;57(3):642-654.

40. Yu JW, Lee MS. Mitochondria and the NLRP3 inflammasome: physiological and pathological relevance. *Arch Pharm Res*. 2016;39(11):1503-1518.

Journal Pre-proof

Journal Pre-proof

Table 1. Analysis of the metal composition in Ni-refining fumes by ICP-MS.

Metal Name	Metal Content (%)
Ni	94.88
Fe	2.41
Cu	1.36
Al	1.28
Others	0.07
Total	100

This experiment was repeated three times. Ni: nickel; ICP-MS: inductively coupled plasma mass spectrometry.

Table 2. A list of primers used in RT-qPCR analysis.

Gene symbol	Forward primer (5' - 3')	Reverse primer (5' - 3')
IL-1β	GAAATGATGGCTTATTACAGTGGCA	GTAGTGGTGGTCGGAGATTCGTAG

TNF-α	CCTGTGAGGAGGACGAACAT	TCGAAGTGGTGGTCTTGTTG
NF-κB(p65)	GGGCACGATTGTCAAAGAT	GGGGACTACGACCTGAATG
caspase-1	GGAATAACGGAGTCAATCA	GACAAGGGTGCTGAACAA
NLRP3	GGGTTTACTGGAGTACCTTTCGAGA	CAGTCGTGTGTAGCGTTTGTTGA
β-actin	TTGCCGACAGGATGCAGAA	GCCGATCCACACGGAGTACT

RT-qPCR: real-time quantitative polymerase chain reaction. IL-1β: interleukin-1β; TNF-α: tumor necrosis factor-α; NF-κB (p65): nuclear factor-κB; NLRP3: NACHT-LRR-PYD domains-containing protein 3.

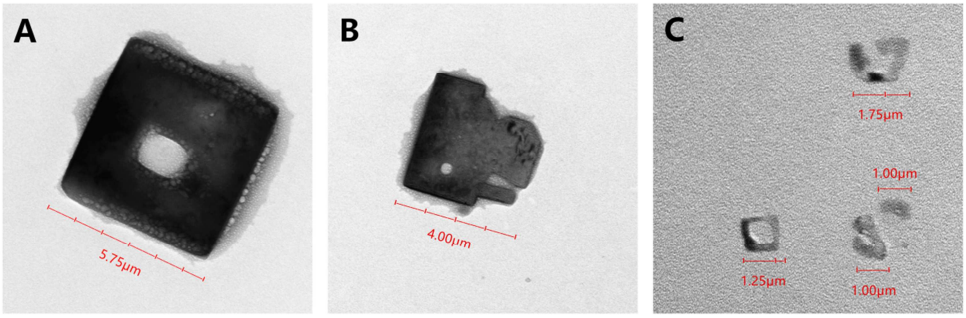

Figure 1. Characterization of Ni-refining fumes shot by transmission electron microscope. (A) 25,000×; **(B)** 25,000×; **(C)** 65,000×**.**

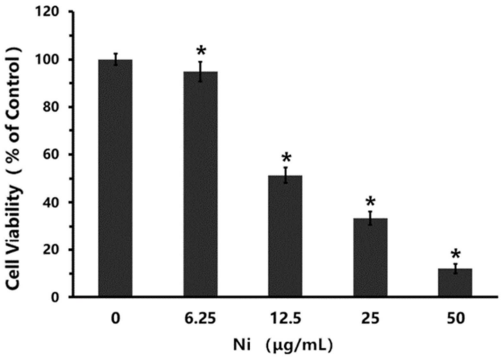

Figure 2. Ni-refining fumes induce cytotoxicity in Beas-2B cells. Data are representative of at least six independent experiments and are presented as mean ± SEM. Compared with the control group, $^{*}P<0.05$.

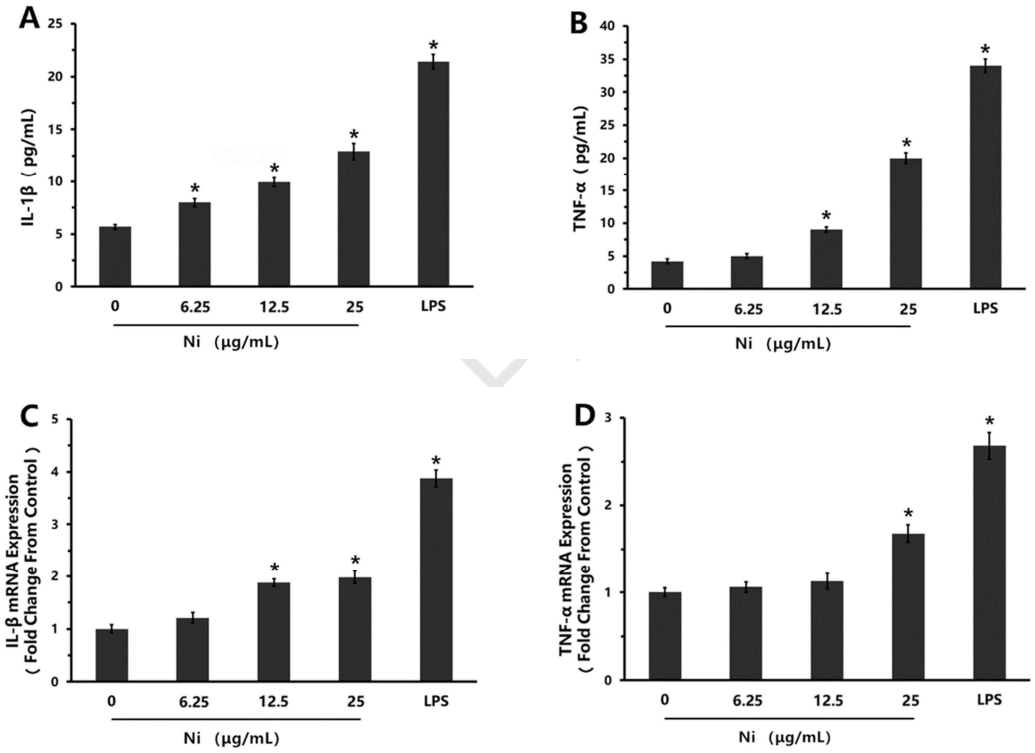

Figure 3. Ni-refining fumes induce cytokine secretion in Beas-2B cells. (A) The expression of IL-1β; **(B)** The expression of TNF-α; **(C)** The expression of IL-1β mRNA; **(D)** The expression of TNF-α mRNA. Data are representative of at least three independent experiments and are presented as mean ± SEM. Compared with the control group, $^{*}P<0.05$.

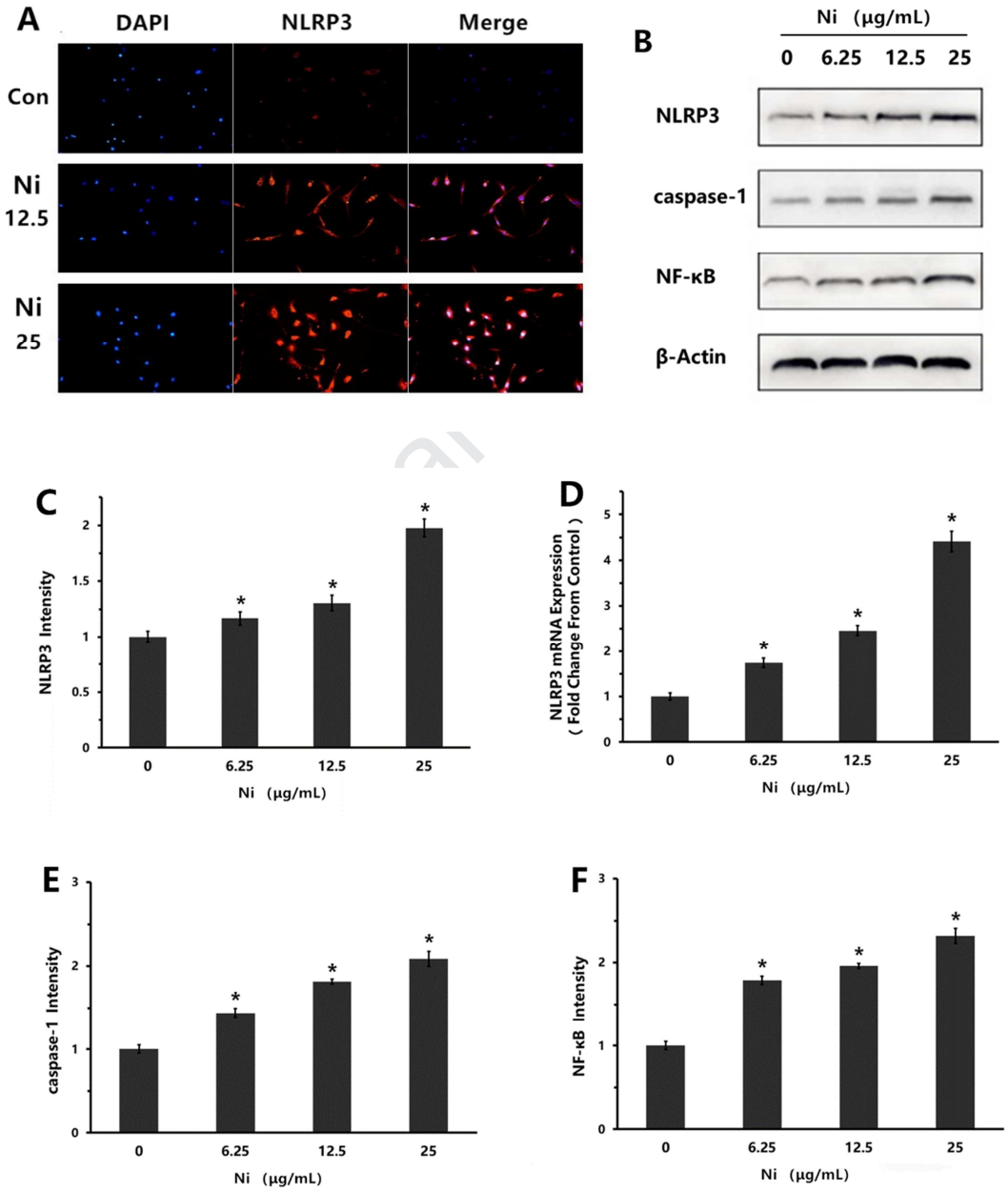

Figure 4. Ni-refining fumes induce NLRP3 inflammasome activation in Beas-2B cells. (A)

The immunofluorescence expression and distribution of NLRP3. (40×). **(B)** Western Blot analysis of NLRP3 inflammasome protein; **(C)** The expression of NLRP3; **(D)** The expression of NLRP3 mRNA; **(E)** The expression of caspase-1; **(F)** The expression of NF-κB (p65); Data are representative of at least three independent experiments and are presented as mean ± SEM. Compared with the control group, $^{*}P<0.05$.

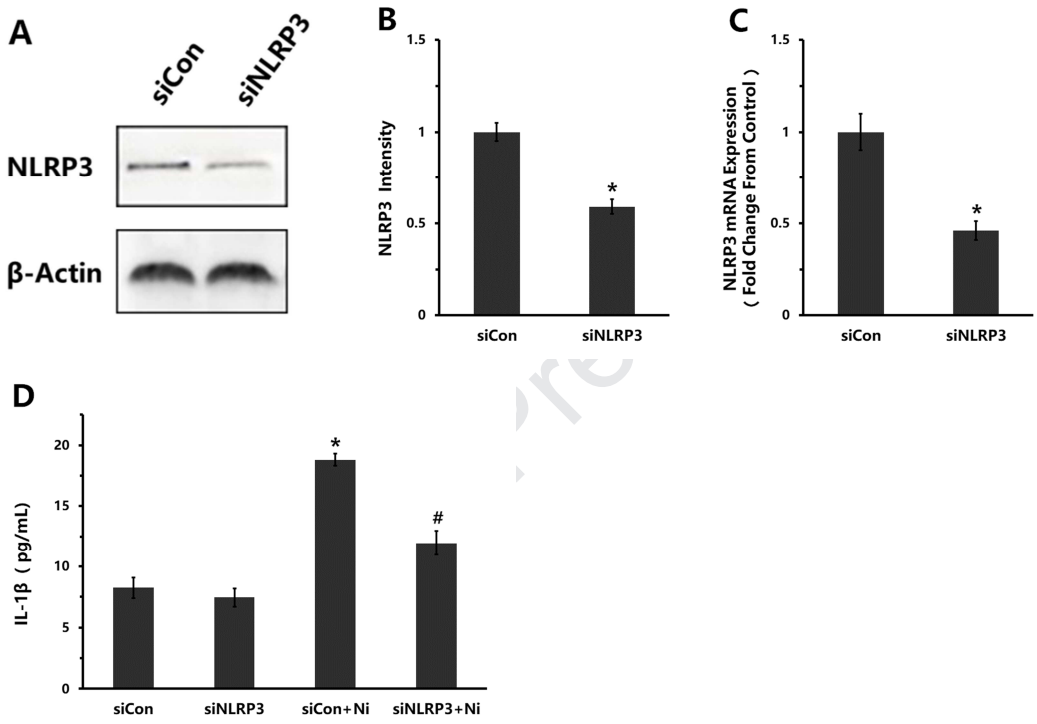

Figure 5. Ni-refining fumes-induced cytokine secretion is dependent on NLRP3 inflammasome activation in Beas-2B cells. (A) Western Bolt analysis of siNLRP3; **(B)**The expression of NLRP3; **(C)** The expression of NLRP3 mRNA; **(D)** The expression of IL-1β; Data are representative of at least three independent experiments and are presented as mean ± SEM. Compared with siCon group, $^{*}P<0.05$; Compared with siCon+Ni group, $^{\#}P<0.05$.

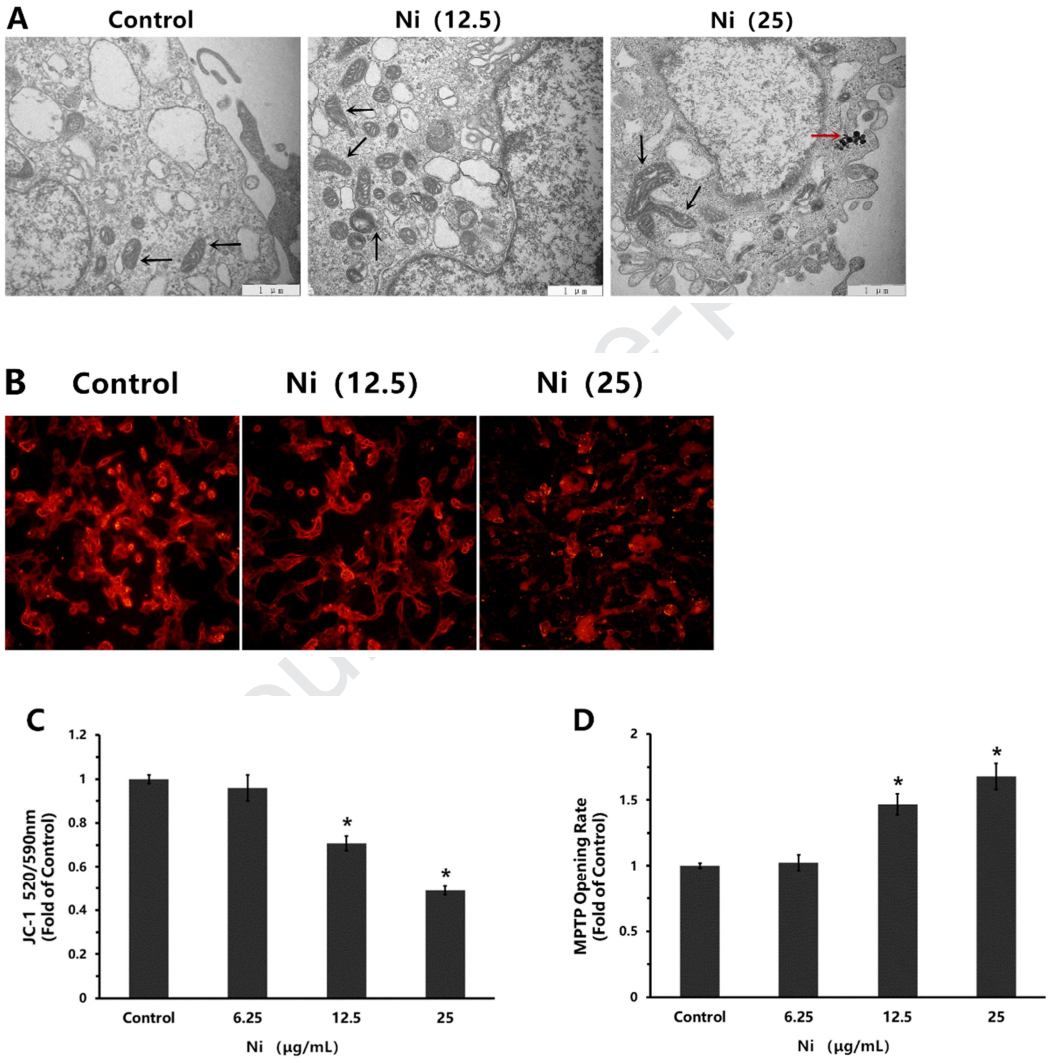

Figure 6. Ni-refining fumes induced mitochondria damage in Beas-2B cells. (A) The change of mitochondria shot by transmission electron microscopy (20,000×). Black arrow mark pointing to mitochondria, red arrow mark pointing to the particles of Ni-refining fumes phagocytosed into the Beas-2B cells. **(B)** The change of MMP relative fluorescence ratio; **(C)** The change of MMP

red fluorescence intensity (40×); **(D)** The change of MPTP relative open rate; Data are representative of at least three independent experiments and are presented as mean ± SEM. Compared with control group, $^{*}P<0.05$.

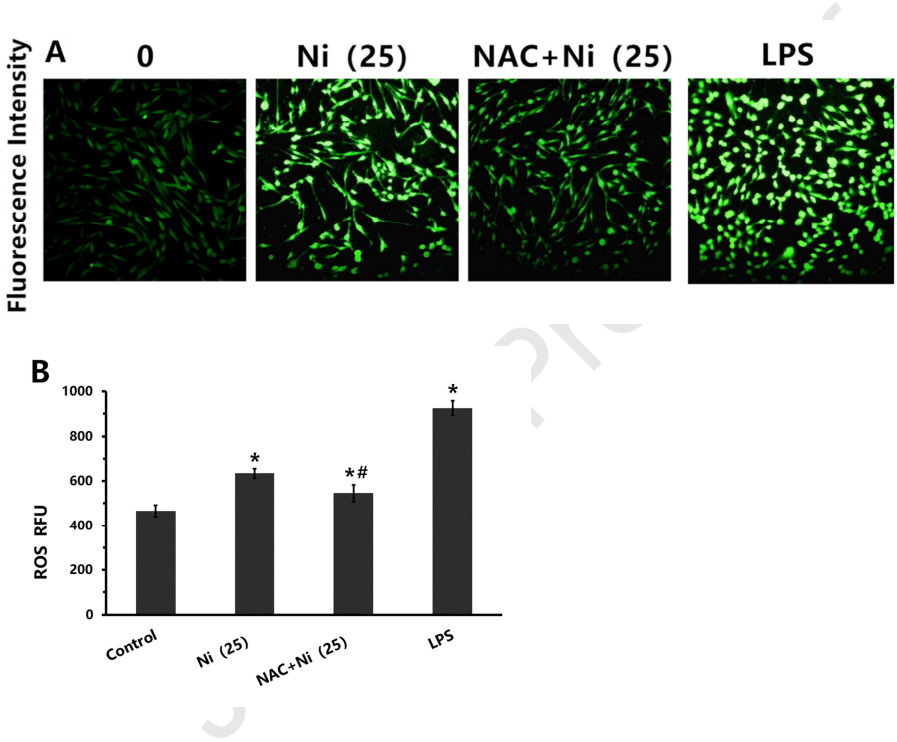

Figure 7. Ni-refining fumes induced ROS production in Beas-2B cells. (A) The change of ROS fluorescence intensity (40×); **(B)** The change of ROS relative fluorescence units. Data are representative of at least three independent experiments and are presented as mean ± SEM. Compared with control group, $^{*}P<0.05$; Compared with 25.00 μg/mL Ni-refining fumes group, $^{\#}P<0.05$.

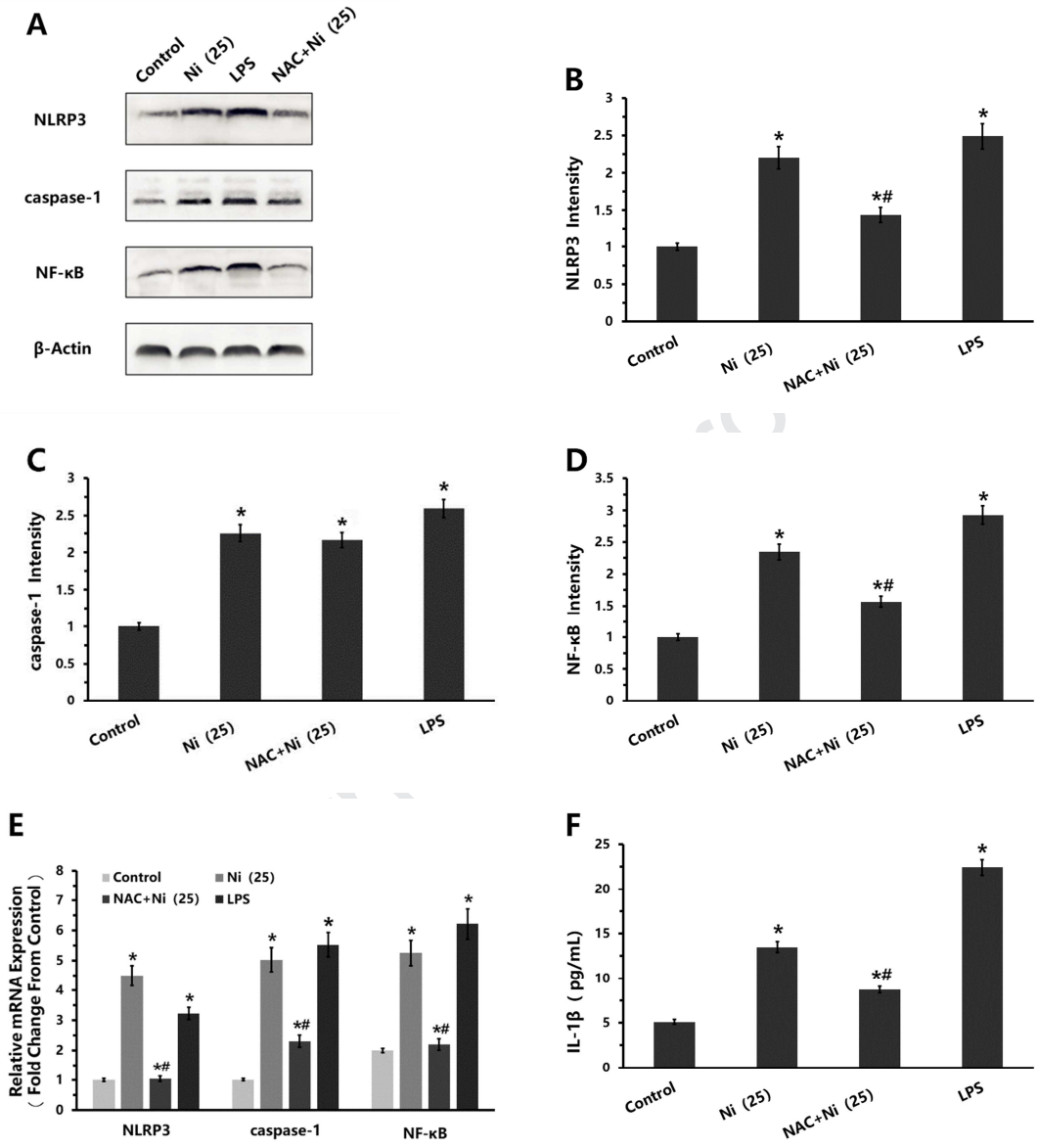

Figure 8. NLRP3 activation by Ni-refining fumes is dependent on ROS production in Beas-2B cells. (A) Western Bolt analysis of NLRP3 inflammasome proteins; **(B)** The expression of NLRP3; **(C)** The expression of caspase-1; **(D)** The expression of NF-κB (p65); **(E)** The expression of NLRP3, caspase-1 and NF-κB (p65) mRNA; **(F)** The expression of IL-1β; Data are representative of at least three independent experiments and are presented as mean ± SEM. Compared with control group, $^{*}P<0.05$; Compared with 25.00 μg/mL Ni-refining fumes group,

$^{\#}P<0.05$.

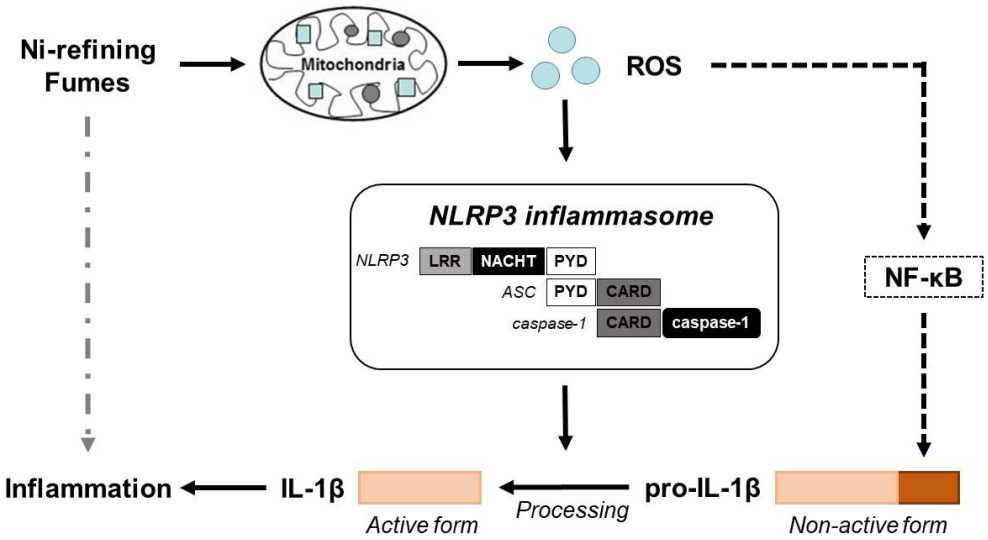

Figure 9. Nickel-refining fumes induce NLRP3 activation dependent on mitochondrial damage and ROS production in Beas-2B cells. Ni-refining fumes can affect the functions of mitochondria, such as changing the level of the MMP, increasing the opening rate of the MPTP, and the resulting ROS overproduction is the most likely signal to activate the NLRP3 inflammasome. The activated NLRP3 inflammasome can process and release IL-1β to induced inflammation in Beas-2B cells eventually.